

Piezoelectric properties and hardening behavior of $K_{5.4}Cu_{1.3}Ta_{10}O_{29}$ -doped $K_{0.5}Na_{0.5}NbO_3$ ceramics

Dunmin Lin,^{1,2,a)} K. W. Kwok,¹ and H. L. W. Chan¹

¹Department of Applied Physics and Materials Research Centre, The Hong Kong Polytechnic University, Kowloon, Hong Kong, People's Republic of China

²College of Chemistry and Materials Science, Sichuan Normal University, Chengdu 610066, People's Republic of China

(Received 27 September 2007; accepted 14 January 2008; published online 20 March 2008)

Lead-free piezoelectric ceramics $K_{0.5}Na_{0.5}NbO_3+x$ mol % $K_{5.4}Cu_{1.3}Ta_{10}O_{29}$ have been prepared by a conventional ceramic fabrication technique. All the ceramics possess a perovskite structure with orthorhombic symmetry. Our results reveal that the addition of $K_{5.4}Cu_{1.3}Ta_{10}O_{29}$ is effective in improving the densification of the ceramics. Besides, after the addition of $K_{5.4}Cu_{1.3}Ta_{10}O_{29}$, the Curie temperature and the tetragonal-orthorhombic phase transition temperature decrease and the P - E loop becomes constricted, in particular, for the ceramic with $x=0.75$. Based on the symmetry-conforming principle of point defects, it is suggested that defect dipoles are formed by the acceptor dopant ions Cu^{2+} and O^{2-} vacancies along the polarization direction. As a result of the low migration rate of defects, the defect dipoles remain in the original orientation during the P - E loop measurement and thus provide restoring forces to reverse the switched polarizations. Similarly, the defect dipoles do not response along with the polarization in the normal piezoelectric activities and thus provide "pinning" to the deformed polarization, making the ceramics become "hardened." For the ceramic with $x=0.75$, the mechanical quality factor Q_m becomes maximum at a value of 1530, while the other piezoelectric properties remain reasonably high: piezoelectric coefficient $d_{33}=90$ pC/N, planar and thickness mode electromechanical coupling factors $k_p=41$ and $k_t=46\%$.
© 2008 American Institute of Physics. [DOI: 10.1063/1.2896588]

I. INTRODUCTION

Lead zirconate titanate (PZT) and PZT-based ceramics have been widely used in electronic and microelectronic devices because of their superior dielectric and piezoelectric properties. However, because of the toxicity of lead oxide, the use of lead-containing ceramics has caused serious environmental problems. Therefore, it is necessary to develop lead-free piezoelectric ceramics with good piezoelectric properties for replacing the lead-containing ceramics in various applications.

In the past several years, much attention has been paid to the alkaline niobate-based materials, and especially to the potassium sodium niobate $K_{0.5}Na_{0.5}NbO_3$ (KNN) family. KNN is one of the most promising candidates for lead-free piezoelectric ceramics because of its high Curie temperature (about 420 °C) and large electromechanical coupling factors.^{1,2} However, it is very difficult to obtain dense KNN ceramics because of the high volatility of alkaline elements at high temperatures. A number of studies have been extensively carried out to improve the sinterability and electrical properties of the ceramics; these include the formation of solid solutions of KNN with other ABO_3 -type ferroelectrics or nonferroelectrics, e.g., KNN-LiNbO₃,³ KNN-Ba(Ti_{0.95}Zr_{0.05})O₃,⁴ KNN-BaTiO₃,⁵ Li- and Ta-modified KNN,^{6,7} KNN-Li(Nb, Ta, Sb)O₃,⁸ KNN-LiSbO₃,^{9,10} KNN-Bi_{0.5}Na_{0.5}TiO₃,¹¹ and the use of sintering aids,¹²⁻¹⁵ e.g., $K_{5.4}Cu_{1.3}Ta_{10}O_{29}$, CuO, and MnO₂. The introduction of

ABO_3 -type compounds into KNN-based ceramics generally lowers the orthorhombic-tetragonal phase transition, making the orthorhombic and tetragonal phases coexist at room temperature.³⁻¹¹ "Softening" effects such as large increases in the relative permittivity ϵ_r , piezoelectric coefficient d_{33} , and electromechanical coupling factors k , have been observed in the ABO_3 -modified KNN-based ceramics with compositions near the coexistence zone of the orthorhombic and tetragonal phases. However, those ceramics usually have a relatively low mechanical quality factor Q_m ($\sim 40-50$).^{3-11,16} Although the KNN-based ceramics have been extensively studied, there is a few work reporting an improvement of Q_m for the ceramics. It has been known that piezoelectric ceramics with high Q_m (i.e., "hard" piezoelectric ceramics) are essential for the high-power and high-voltage applications, such as ultrasonic microbender and transformers. Therefore, there is great interest and need to develop hard lead-free piezoelectric ceramics for these applications.

Recently, it has been shown that the addition of $K_{5.4}Cu_{1.3}Ta_{10}O_{29}$ (KCT) is effective in enhancing the densification and increasing Q_m of KNN ceramics.¹² However, there were no systematic investigations on the "hardening" effects of KCT on the ceramics.¹² In this work, KCT-doped KNN ceramics were prepared by an ordinary solid-state sintering method, and their structure, dielectric, ferroelectric, and piezoelectric properties were studied in detail. The origin for the hardening effects was also discussed.

^{a)}Electronic mail: ddmd222@yahoo.com.cn.

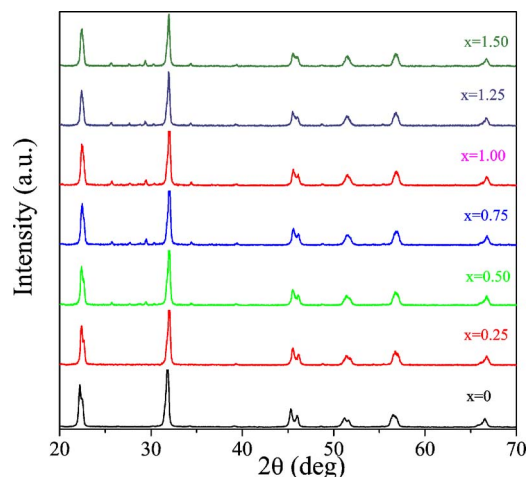


FIG. 1. (Color online) XRD patterns of the KNN-KCT- x ceramics.

II. EXPERIMENTAL

A conventional ceramic fabrication technique was used to prepare $\text{K}_{0.5}\text{Na}_{0.5}\text{NbO}_3 + x$ mol % $\text{K}_{5.4}\text{Cu}_{1.3}\text{Ta}_{10}\text{O}_{29}$ (abbreviated as KNN-KCT- x) ceramics using analytical-grade metal oxides or carbonate powders: Na_2CO_3 (99.8%), K_2CO_3 (99.9%), Nb_2O_5 (99.95%), Ta_2O_5 (99.9%), and CuO (99%). The stoichiometric KNN and KCT powders were first synthesized at 880 °C for 6 h and 950 °C for 5 h, respectively, by a solid-state reaction method. After the calcination, KNN and KCT powders were weighted according to the formula of KNN-KCT- x and ball milled for 8 h. The resulting mixture was further mixed with a polyvinyl alcohol binder solution thoroughly and then pressed into disk samples. The disk samples were sintered at 1100–1110 °C for 4 h in air. Silver electrodes were fired on the top and bottom surfaces of the sintered samples. The ceramics were poled under a dc field of 5–6 kV/mm at 200 °C in a silicon oil bath for 30 min.

The crystalline structure of the sintered samples was examined using x-ray diffraction (XRD) analysis with $\text{Cu K}\alpha$ radiation (Bruker D8 advance). The microstructure was observed using a scanning electron microscopy (Leica Ste-

reoscan 440). The relative permittivity ϵ_r and loss tangent $\tan \delta$ at 1, 10, and 100 kHz were measured as a function of temperature using an impedance analyzer (Agilent 4192A). A conventional Sawyer–Tower circuit was used to measure the polarization hysteresis (P - E) loop at 100 Hz. The electromechanical coupling factors k_p and k_t and mechanical quality factor Q_m were determined by the resonance method according to the IEEE Standard 176 using an impedance analyzer (Agilent 4294A). The piezoelectric coefficient d_{33} was measured using a piezo- d_{33} meter (ZJ-3A, China).

III. RESULTS AND DISCUSSION

Figure 1 shows the XRD patterns of the KNN-KCT- x ceramics. All of the ceramics exhibit a perovskite structure with orthorhombic symmetry. At $x < 0.50$, the ceramics possess a single phase. A small amount of KCT and $\text{KTa}_5\text{O}_{13}$ phases are observed in the ceramics with $x > 0.50$. There are no significant differences between the diffraction patterns of the ceramics, suggesting that the KNN-KCT- x ceramics should be a normal ferroelectric.

The scanning electron microscopy (SEM) micrographs of the KNN-KCT- x ceramics with $x = 0, 0.25, 0.75$, and 1.50 are shown in Fig. 2. For the pure KNN ceramic (i.e., $x = 0$), the grains have a diameter in the range of 1–1.5 μm , and a small amount of pores is observed [Fig. 2(a)]. The relative density (determined by the Archimedes method) of the ceramic is low (about 92%). With the increase of x to 0.75, the grains become smaller and more uniform [Figs. 2(b) and 2(c)]. The ceramics are denser and almost no pores are observed, thus giving a larger relative density (>96%). These results clearly show that the addition of KCT can improve the sintering performance of the ceramics. It is suggested that KCT may settle at the grain boundaries and reduce their mobility during the densification. As a result, the mass transportation becomes weakened and the grain growth is inhibited, thereby producing grains of smaller and uniform size. At $x = 1.50$ (excess KCT), there are distinct grains of diameter about 7.5 μm uniformly distributed among the grains which are of much smaller diameters, about 1.5 μm [Fig.

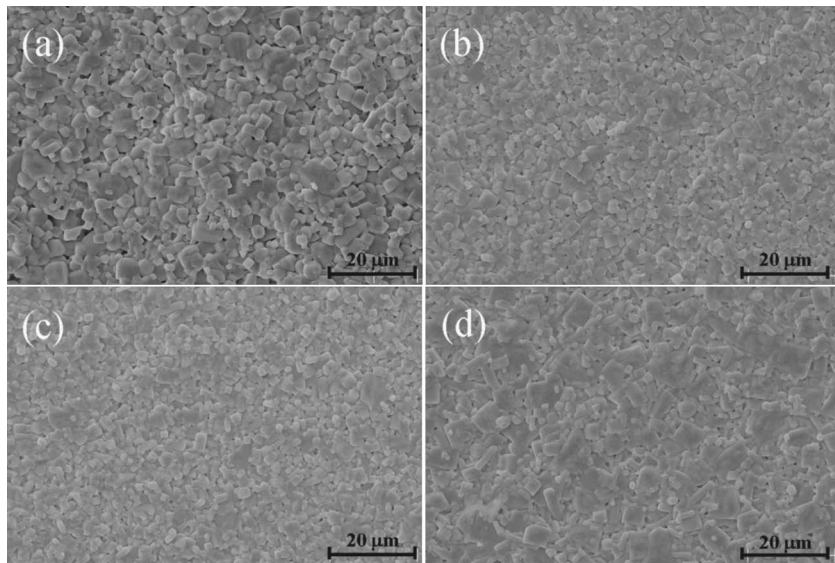


FIG. 2. SEM micrographs of the KNN-KCT- x ceramics: (a) $x = 0.00$, sintered at 1100 °C for 4 h; (b) $x = 0.25$, sintered at 1110 °C for 4 h; (c) $x = 0.75$, sintered at 1110 °C for 4 h; and (d) $x = 1.50$, sintered at 1110 °C for 4 h.

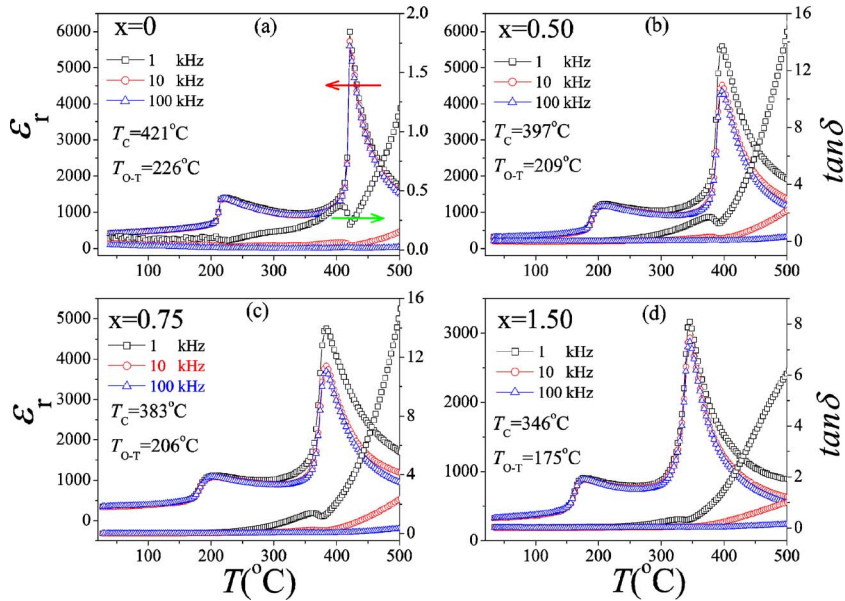


FIG. 3. (Color online) Temperature dependences of ϵ_r and $\tan \delta$ at 1, 10, and 100 kHz for the KNN-KCT- x ceramics with $x=0, 0.50, 0.75,$ and 1.50 .

2(d)]. The abnormal grain growth in the KNN-KCT-1.50 ceramic may be attributed to the formation of a liquid phase [Fig. 2(d)] resulting from the low melting temperatures of the Cu-containing compounds.

The temperature dependences of ϵ_r and $\tan \delta$ for the KNN-KCT- x ceramics with $x=0, 0.50, 0.75,$ and 1.50 are shown in Fig. 3. Similar to a pure KNN ceramic, all of the KNN-KCT- x ceramics undergo two phase transitions: the paraelectric cubic-ferroelectric tetragonal phase transition at T_C and the ferroelectric tetragonal-ferroelectric orthorhombic phase transition at T_{O-T} . As x increases, both the observed T_C and T_{O-T} decrease and the dielectric peak at T_C becomes slightly broadened. These should be attributed to the substitution of Ta^{5+} for the B -site ion Nb^{5+} in the KNN ceramics.^{7,12} Because of the similar ionic radii, Cu^{2+} (0.73 \AA) may substitute Nb^{5+} (0.68 \AA) as an acceptor dopant, which may also lead to a slight decrease in T_{O-T} .¹⁴

Figure 4 shows the P - E loops for the as-sintered KNN-KCT- x ceramics with $x=0, 0.50, 0.75, 1.00, 1.25,$ and 1.50 at 100 Hz. At $x=0$, the ceramic exhibits a well-saturated and squarelike P - E loop with a saturation polarization (P_s) of $25 \mu\text{C}/\text{cm}^2$ and a remnant polarization (P_r) of $20 \mu\text{C}/\text{cm}^2$.

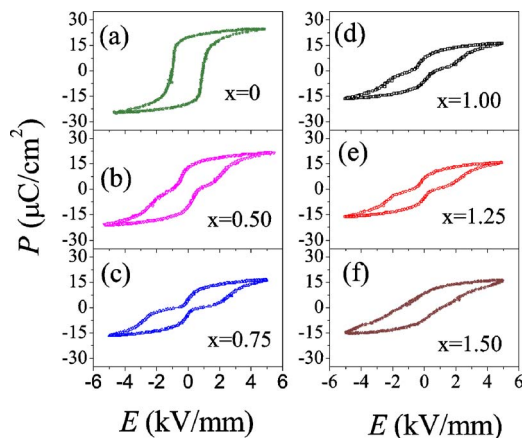


FIG. 4. (Color online) P - E loops of the KNN-KCT- x ceramics with $x=0, 0.50, 0.75, 1.00, 1.25,$ and 1.50 at 100 Hz.

As x increases, the P - E loop becomes slanted and constricted, giving smaller values of P_s and P_r . It can be seen that the P - E loop for the KNN-KCT-0.75 ceramic is the most constricted, revealing a double-loop-like characteristics. On the basis of the results on the crystalline structure and phase transitions, it could conclude that the KNN-KCT- x ceramics (with $x \neq 0$) should not be antiferroelectrics. The double-loop-like characteristics may hence be caused by the pinning of ferroelectric domains by defects.

It has been shown that after aging, a number of ferroelectric titanates will exhibit a double P - E loop.¹⁷⁻¹⁹ It is generally believed that the double P - E loop is caused by a constriction of the polarization, which may be resulted from the stabilization of ferroelectric domains by defects. Various stabilization theories such as the grain-boundary theory, surface-layer model, domain-wall theory, and volume theory have been proposed.²⁰ Recently, based on the symmetry-conforming principle of point defects, Ren has shown that the domain stabilization is a volume effect.^{17-19,21} Although the mechanism was proposed based on the experimental observations on acceptor-doped BaTiO_3 ceramics, it is also applicable to other perovskite ferroelectrics, such as acceptor-doped KNN and KNbO_3 ceramics.^{14,22} After the substitution of Cu^{2+} for the B -site ions Nb^{5+} , O^{2-} vacancies are formed in the KNN-KCT- x ceramics (with $x \neq 0$). In the ferroelectric state, the B -site ion is not located in the center of the oxygen octahedral. As a result, the (statistical) distribution of O^{2-} vacancies around a dopant ion Cu^{2+} is not symmetric and affected strongly by the lattice symmetry. At equilibrium, the symmetry of short-range order distribution of defects (or defect symmetry) follow the polar crystal symmetry of KNN.¹⁷⁻¹⁹ The resulting noncentric distribution of defects (positively charged O^{2-} vacancies and negatively charged dopant ions Cu^{2+}) forms defect dipoles along the spontaneous polarization direction. In the P - E loop measurements, the polarization is switched (abruptly) by the external field. Probably due to insufficient time for the vacancies to migrate (at room temperature), the defect dipoles remain in the origi-

nal orientation, thus providing a restoring force to reverse the switched polarization upon removal of the external field.

Unlike BaTiO₃, aging is not required for the KNN-KCT-0.75 ceramic to correct the defect symmetry into the polar orthorhombic symmetry and then to exhibit the double-loop-like characteristics. The aging time for BaTiO₃ is usually long, e.g., 5 days at 80 °C or 28 days at room temperature.¹⁷⁻¹⁹ Apparently, the two ceramics undergo different phase transitions during the cooling from the sintering temperature. BaTiO₃ undergoes a cubic-tetragonal phase transition at ~128 °C, while the KNN-KCT-0.75 ceramic undergoes the cubic-tetragonal phase transition at 383 °C, and then the tetragonal-orthorhombic phase transition at 206 °C. Although the tetragonal-orthorhombic phase transition for the KNN-based ceramics is a diffuse phase transition,²³ it is of the same nature as the cubic-tetragonal phase transition, i.e., it is a crystal transformation arising from the shift of ions. It is hence suggested that the transition temperature should be the key parameter determining the requirement for aging. The migration rate of the defects (O²⁻ vacancies) at high temperatures (e.g., 206 °C) is higher, so the defect symmetry of the KNN-KCT-0.75 ceramic can correct almost completely to the polar crystal symmetry after the tetragonal-orthorhombic phase transition. Similar results have been reported for a Cu-doped KNN ceramic.¹⁴ On the other hand, probably due to insufficient time resulting from the slow migration rate, the defect symmetry of the BaTiO₃ remains in the cubic symmetry after the cubic-tetragonal transition at 128 °C and hence additional time (e.g., aging) is required for the defect symmetry to correct to the tetragonal symmetry. This should also be the reason for the KNN-KCT-1.50 ceramic not showing a constricted *P-E* loop [Fig. 4(f)]. The observed T_{O-T} for the ceramic is ~175 °C. Although the KNN-KCT-*x* ceramics with $x < 0.75$ have a high T_{O-T} (>206 °C), there may exist not enough O²⁻ vacancies and hence defect dipoles to constrict the polarization.

To provide additional evidence for the defect migration, the KNN-KCT-0.75 and KNN-KCT-1.50 ceramics were aged at 80 °C for 30 days, and their *P-E* loops are shown in Fig. 5. It can be seen that the *P-E* loop for the KNN-KCT-1.50 ceramic becomes constricted at $E=0$. This clearly indicates that the migration of vacancies has taken place, correcting the defect symmetry to the tetragonal symmetry. Similar aging effect on KNbO₃-based ceramics has also been reported recently by Feng and Ren.²² It can be seen that there is no significant difference between the *P-E* loops of the as-sintered and aged KNN-KCT-0.75 ceramic, suggesting that almost all the vacancies have migrated and settled in the polar crystal symmetry after the fabrication process.

The variations of d_{33} , k_t , k_p , ϵ_r , $\tan \delta$, and Q_m with x for the KNN-KCT- x ceramics are shown in Fig. 6. The observed k_p and k_t remain almost unchanged at a value of 41% and 46%, respectively, after the addition of KCT, and then decrease at $x > 1.0$. The d_{33} , ϵ_r , and $\tan \delta$ decrease as x increases from 0 to 0.25, and then remain almost unchanged at a value of 90 pC/N, 330, and 0.30%, respectively. Unlike other material parameters, Q_m exhibits a large dependence on x . As x increases, Q_m increases significantly and then decreases, giving a maximum value of about 1530 at $x=0.75$. It is sug-

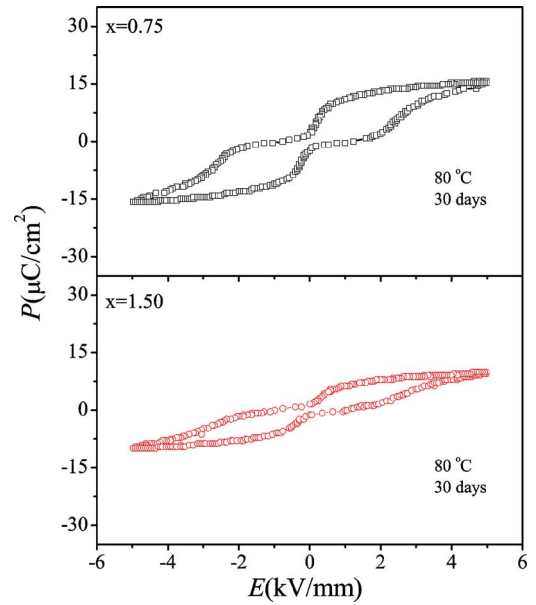


FIG. 5. (Color online) *P-E* loops of the KNN-KCT-0.75 and KNN-KCT-1.50 ceramics at 100 Hz after aging at 80 °C for 30 days.

gested that, because of the low migration rate at room temperature, the defect dipoles do not respond along with the polarization during the normal piezoelectric activities (i.e., expands and contracts continuously), and thus providing a restoring force or pinning to the deformed polarization. As a result, the mechanical quality factor is increased and the ceramics become hardened.

The impedance magnitude $|Z|$ and phase angle θ as a function of frequency for the KNN-KCT- x ceramics with $x = 0.00, 0.50, 1.00,$ and 1.50 at the planar-mode resonance are shown in Fig. 7. It can be seen that, because of the high Q_m , the KNN-KCT-0.50 and KNN-KCT-1.00 ceramics exhibit a very squarelike resonance peak. This is in agreement with the observations for other hard piezoelectric ceramics, e.g., PZT-8 [which has a Q_m of 900 (Ref. 24)].

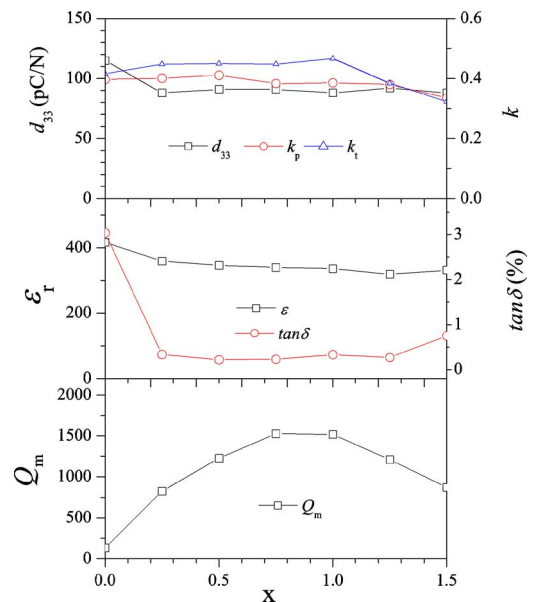


FIG. 6. (Color online) Variations of d_{33} , k_t , k_p , ϵ_r , $\tan \delta$, and Q_m with x for the KNN-KCT- x ceramics.

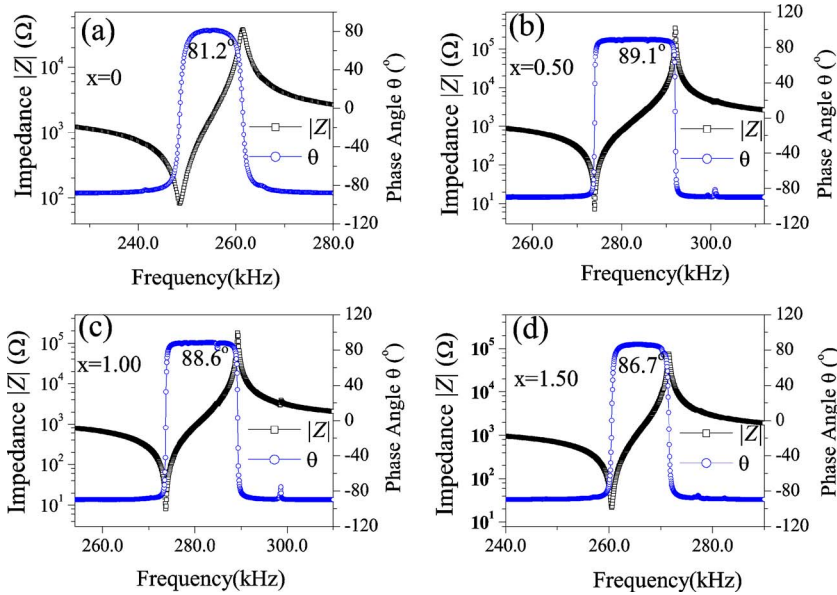


FIG. 7. (Color online) Frequency dependences of impedance $|Z|$ and phase angle θ for the KNN-KCT- x ceramics with $x=0, 0.50, 1.00$, and 1.50 at the planar-mode resonance.

IV. CONCLUSIONS

KNN-KCT- x lead-free ceramics have been prepared by a conventional ceramic fabrication technique. All the ceramics possess a perovskite structure with orthorhombic symmetry. The addition of KCT can improve the densification of the ceramics effectively. Besides, after the addition of KCT, the observed T_C and T_{O-T} decrease and the P - E loop becomes constricted, in particular, for the KNN-KCT-0.75 ceramic. It is suggested that, because of the symmetry-conforming property, the acceptor dopant ions Cu^{2+} and O^{2-} vacancies form defect dipoles along the polarization direction. As a result of the low defect migration rate, the defect dipoles remain in the original orientation during the P - E loop measurement, and thus provide restoring forces to reverse the switched polarizations. Likewise, the defect dipoles provide pinning effects in the normal piezoelectric activities, making the ceramics become hardened. For the KNN-KCT-0.75 ceramic, Q_m becomes maximum at the value of 1530, while the other piezoelectric properties remain reasonably high: $d_{33}=90$ pC/N, $k_p=41\%$, and $k_t=46\%$.

ACKNOWLEDGMENTS

This work was supported by the Niche Area Projects (1-BB95 and 1-BBZ3) and the Centre for Smart Materials of The Hong Kong Polytechnic University.

¹L. Egerton and D. M. Dillom, *J. Am. Ceram. Soc.* **42**, 438 (1959).

²R. E. Jaeger and L. Egerton, *J. Am. Ceram. Soc.* **45**, 209 (1962).

³Y. Guo, K. Kakimoto, and H. Ohsato, *Appl. Phys. Lett.* **85**, 4121 (2004).

⁴D. Lin, K. W. Kwok, and H. W. L. Chan, *Appl. Phys. A: Mater. Sci. Process.* **88**, 359 (2007).

⁵H. Y. Park, C. W. Ahn, H. C. Song, J. H. Lee, S. Nahm, K. Uchino, H. G. Lee, and H. J. Lee, *Appl. Phys. Lett.* **89**, 062906 (2006).

⁶E. Hollenstein, M. Davis, D. Damjanovic, and N. Setter, *Appl. Phys. Lett.* **87**, 182905 (2005).

⁷D. Lin, K. W. Kwok, and H. W. L. Chan, *J. Appl. Phys.* **102**, 034102 (2007).

⁸Y. Saito, H. Takao, T. Tani, T. Nonoyama, K. Takatori, T. Homma, T. Nagaya, and M. Nakamura, *Nature (London)* **432**, 84 (2004).

⁹D. Lin, K. W. Kwok, and H. W. L. Chan, *J. Appl. Phys.* **101**, 074111 (2007).

¹⁰S. Zhang, R. Xia, T. R. Shout, G. Zhang, and J. Wang, *J. Appl. Phys.* **100**, 104108 (2006).

¹¹R. Zuo, X. Fang, and C. Ye, *Appl. Phys. Lett.* **90**, 092904 (2007).

¹²M. Matsubara, K. Kikuta, and S. Hirano, *J. Appl. Phys.* **97**, 114105 (2005).

¹³H. Takao, Y. Saito, Y. Aoki, and K. Horibuchi, *J. Am. Ceram. Soc.* **89**, 1951 (2006).

¹⁴D. Lin, K. W. Kwok, and H. W. L. Chan, *Appl. Phys. Lett.* **90**, 232903 (2007).

¹⁵S. H. Park, C. W. Ahn, S. Nahm, and J. S. Song, *Jpn. J. Appl. Phys., Part 2* **43**, L1072 (2004).

¹⁶T. R. Shrotr and S. J. Zhang, *J. Electroceram.* **19**, 113 (2007).

¹⁷X. Ren, *Nat. Mater.* **3**, 91 (2004).

¹⁸L. X. Zhang, W. Chen, and X. Ren, *Appl. Phys. Lett.* **85**, 5658 (2004).

¹⁹W. Liu, W. Chen, L. Yang, L. Zheng, Y. Wang, C. Zhou, S. Li, and X. Ren, *Appl. Phys. Lett.* **89**, 172908 (2006).

²⁰P. V. Lambeck and G. H. Jonker, *J. Phys. Chem. Solids* **47**, 453 (1986).

²¹L. Zhang and X. Ren, *Phys. Rev. B* **73**, 094121 (2006).

²²Z. Feng and X. Ren, *Appl. Phys. Lett.* **91**, 032904 (2007).

²³D. H. Cho, M. K. Ryu, S. S. Park, S. Y. Cho, J. G. Choi, M. S. Jang, J. P. Kim, and C. R. Cho, *J. Korean Phys. Soc.* **46**, 151 (2005).

²⁴http://www.piezo-kinetics.com/Navy_Type_III.htm